tvst

Article

Clinical Evaluations of Macular Structure-Function Concordance With and Without Drasdo Displacement

Janelle Tong[1,2], Jack Phu[1,2], David Alonso-Caneiro[3], Sieu K. Khuu[2], and Michael Kalloniatis[1,2]

[1] Centre for Eye Health, University of New South Wales (UNSW), Sydney, New South Wales, Australia
[2] School of Optometry and Vision Science, University of New South Wales (UNSW), Sydney, New South Wales, Australia
[3] Queensland University of Technology, Contact Lens and Visual Optics Laboratory, Centre for Vision and Eye Research, School of Optometry and Vision Science, Queensland, Australia

Correspondence: Michael Kalloniatis, School of Optometry and Vision Science, University of New South Wales (UNSW), Sydney 2052, New South Wales, Australia.
e-mail: m.kalloniatis@unsw.edu.au

Received: December 6, 2021
Accepted: March 27, 2022
Published: April 19, 2022

Keywords: glaucoma; structure-function relationship; macula; optical coherence tomography; visual field

Citation: Tong J, Phu J, Alonso-Caneiro D, Khuu SK, Kalloniatis M. Clinical evaluations of macular structure-function concordance with and without drasdo displacement. Transl Vis Sci Technol. 2022;11(4):18, https://doi.org/10.1167/tvst.11.4.18

Purpose: The purpose of this study was to compare concordance between ganglion cell-inner plexiform layer (GCIPL) data from the Cirrus optical coherence tomographer (OCT) Ganglion Cell Analysis (GCA) and visual fields (VFs), with and without Drasdo displacement.

Methods: From 296 open-angle glaucoma participants, GCIPL deviation and raw thickness data were extracted over locations per the 10-2 VF test grid, with and without application of Drasdo displacement, with global and eccentricity-dependent sensitivities and specificities calculated for both. With OCT and VF data classified as within or outside normative limits, pattern deviation values were compared using paired *t*-tests and Spearman correlations. Regression models were applied to pattern deviation values as a function of GCIPL thickness, and differences in model performance with and without displacement were compared using extra sums-of-squares F tests.

Results: There were small but significant improvements in global specificity without displacement (0.58–0.59 with displacement and 0.61 without displacement), without notable differences in sensitivity (0.77–0.78 with displacement and 0.76–0.78 without displacement). At abnormal VF locations and without displacement, a higher proportion of correct OCT classifications ($P = 0.0008$) and significant correlation with worsening pattern deviation values were observed ($r = 0.50$, $P = 0.002$). Regression models indicated significantly steeper slopes with Drasdo displacement centrally ($P = 0.002$–0.04).

Conclusions: With GCA deviation maps, small improvements in structure-function concordance were observed without displacement, which are unlikely to be clinically meaningful. Using GCIPL thickness data, significantly better structure-function concordance was observed centrally with Drasdo displacement.

Translational Relevance: Applying Drasdo displacement on probability-based reports is unlikely to alter clinical impressions of structure-function concordance, but applying displacement with GCIPL thickness data may improve detection of structure-function concordance.

Introduction

Glaucoma is a progressive optic neuropathy manifesting as defects to the optic nerve head and its projections to the retinal nerve fibers and ganglion cells (RGCs), and is typically accompanied by characteristic corresponding defects in the visual field (VF).[1] Typical investigations for glaucoma include slit-lamp biomicroscopy, measurement of intraocular pressure, gonioscopic evaluation of the angular structures, funduscopic examination, and quantitative measurements of ocular structures using optical coherence tomography (OCT) and VFs using static automated perimetry (SAP), respectively. From this battery of tests, should a defect to the optic nerve head and its projections seen

on structural examination be observed with a corresponding functional defect, or if structure-function concordance is observed, this generally confers greater confidence in a diagnosis of glaucoma.[2,3] However, overlap between conventional testing areas and therefore the ability to directly compare structural data from OCT and functional data from SAP is currently limited to the macular region. Nonetheless, assessment of the macular structure-function relationship remains highly relevant in glaucoma, given the potential for macular involvement even in early stages of glaucoma and its associated visual morbidity.[4–7]

To complicate comparisons of macular structure and function in glaucoma, central RGCs are laterally displaced from their underlying photoreceptors, and subsequently their receptive fields, due to Henle's fibers.[8] As such, many studies investigating the glaucomatous macular structure-function relationship have extracted OCT measurement locations under consideration of RGC displacement, using models such as the Drasdo displacement model,[8] to theoretically enable precise comparisons of colocalized structure and function.[9–13] Unfortunately, this additional step is not performed on many commercially available software collating OCT and VF information, with the exception of the Hood Report on Spectralis OCT (Heidelberg Engineering, Heidelberg, Germany). Theoretically, this limits the anatomic accuracy of clinical judgments regarding macular structure-function concordance.

However, previous investigations have reported significantly better concordance between macular OCT and 10-2 VFs without displacement of OCT measurements corresponding to VF stimulus locations.[14] In turn, this suggests that the additional precision in extracting OCT measurements considering RGC displacement may not significantly alter interpretation of presence or absence of structure-function concordance in clinical settings. As these findings appear to oppose methodology routinely applied in research settings, further investigation would be valuable to identify whether the additional step of applying theoretical RGC displacement to clinical OCT data improves clinical judgment of macular structure-function concordance.

In this study, a head-to-head comparison of macular structure-function concordance with and without consideration of anatomic displacement was conducted, by comparing OCT measurements from the Cirrus HD-OCT (Carl Zeiss Meditec Inc., Dublin, CA) extracted over displaced RGC locations versus without displacement to VF results at corresponding locations as the "clinical the period should be outside the quote." The findings of this study aim to shed light on the relevance of RGC displacement to clinically obtained OCT measurements in comparison to functional data, in turn guiding appropriate methods for improving clinical appraisals of macular structure-function concordance.

Methods

Participant Recruitment

Participants were retrospectively recruited from patients attending the Centre for Eye Health (Sydney, Australia). All participants had previously provided written consent for their clinical data to be used for research purposes per protocols approved by the University of New South Wales Australia Human Research Ethics Advisory panel. This study adhered to the tenets of the Declaration of Helsinki.

In line with clinical protocols at the Centre for Eye Health,[15] all patients diagnosed with or suspected of having glaucoma undergo comprehensive examinations, including slit-lamp biomicroscopy, central corneal thickness measurement (Pachmate; DGH Technology Inc., Exton, PA), applanation tonometry, gonioscopic examination of the anterior chamber angle, dilated funduscopic examination, optic nerve and macula imaging with the Cirrus HD-OCT, and 24-2 Swedish Interactive Threshold Algorithm (SITA) Faster VF testing (Humphrey Field Analyzer; Carl Zeiss Meditec Inc.). Additionally, 10-2 SITA Fast is performed on participants suspected of central VF loss, based on 24-2 VF and/or structural findings. Participants were selected from patients who had been diagnosed with open angle glaucoma in at least 1 eye, for which they were either undergoing treatment with topical medication or had been treated with selective laser trabeculoplasty, and had 10-2 VF testing conducted during their clinical examination. Additional inclusion criteria were no other notable retinal or neurological pathologies that could affect segmentation of OCT scans or retinal thickness measurements, signal strength of OCT scans of 7 or greater, and reliable 10-2 VF results meeting manufacturer-specified criteria of $<20\%$ fixation losses and $<15\%$ false positive results. Where one eye met the above criteria, this eye was included for further analyses, whereas if both eyes were eligible one eye was randomly selected. Participants were consecutively recruited from patients meeting these criteria, with data from 128 participants included in a previous study.[5]

VF Data Extraction

From 10-2 VF results, categorical and continuous data were extracted from pattern deviation

probability and quantitative decibel values, respectively, which were chosen over total deviation and threshold data due to its widespread use in clinical assessments for glaucoma, given its compensation for individual hills of vision enhancing visualization of focal defects.[3] After extraction, all results were converted to right eye format to facilitate interparticipant comparison. Per Hodapp-Parish-Anderson (HPA) criteria,[16,17] individual VF locations were denoted as defective if they fell within a cluster containing at least 3 contiguous points classified as $P < 5\%$ or worse on the pattern deviation probability map, with at least 1 point classified as $P < 1\%$ or worse.

Macular OCT Data Processing

For macular structure-function analyses using readily available clinical data, Ganglion Cell Analysis (GCA) printouts were generated for each participant from Cirrus OCT macular cube scans, and saved as portable networks graphic (PNG) files to preserve pixel-wise color information. The GCA displays ganglion cell-inner plexiform layer (GCIPL) measurements captured across the entire scan area, measuring 6 × 6 mm, with quantitative measurements and comparisons to the inbuilt normative database calculated over an elliptical annulus with outer dimensions of 4.8 × 4.0 mm horizontally and vertically, and inner dimensions of 1.2 × 1.0 mm horizontally and vertically. For preservation of location-specific data, the deviation map was chosen for analyses based on the GCA printout, where GCIPL thickness information is categorized based on percentiles of the normative distribution, with yellow and red pixels indicating data points lower than the fifth and first percentiles, respectively.

The displacement model applied in this study was derived from figure 6 in the study by Drasdo et al.,[8] depicting RGC displacement as a function of cone eccentricity averaged across all principal meridians, which is consistent with many previous studies investigating the macular structure-function relationship.[9–11,13,18] Degree coordinates for the 10-2 VF stimulus centers were converted to millimeters per Drasdo and Fowler,[19] and corresponding displacements were subsequently applied to displace the VF stimulus centers. Circles were drawn around displaced and nondisplaced centers to identify locations over which OCT information would be extracted, with the circle radius of 0.215 degrees matching projected Goldmann III stimulus sizes as used in 10-2 SITA Fast testing. For both displaced and non-displaced locations, only data from locations where entire circles fell consistently within the GCA elliptical annulus were flagged for extraction.

A custom algorithm to extract GCA deviation map probability values from displaced and non-displaced 10-2 VF locations were written using MATLAB version R2019a (Mathworks, Natick, MA; Fig. 1). Each deviation map was flipped vertically to match VF results and converted to right eye format. To ensure accurate centration of the superimposed extraction locations, foveal centers were manually selected via visual inspection. The algorithm extracted averaged color pixel information in RGB format, with a minimum difference in pixel values of 30 required between the red/green and blue values and red and green/blue values for classification at less than the fifth percentile and less than the first percentile, respectively, with any location classified as at least less than the fifth percentile subsequently denoted as defective on OCT.

Although deviations from the normative distribution are commonly used to identify structural defects on OCT, these are not always reflective of underlying GCIPL thickness measurements. For precise extraction of raw GCIPL thickness data, Cirrus OCT macular cube scans were exported in image format (IMG), and GCIPL segmentation was performed using OCT Segmentation version 2.11, an open-source software tool available as part of the Automated Retinal Analysis (AURA) tool (https://www.nitrc.org/projects/aura_tools/; provided in the public domain by Neuroimaging Tools and Resources Collaboration, University of Massachusetts Medical School, Worcester, MA).[20] An additional advantage is that raw GCIPL thickness data can be extracted over the entire OCT scanning area of 6 × 6 mm, enabling comparisons to close to all VF data from the 10-2 test grid. GCIPL thickness maps were flipped vertically to match VFs and converted to right eye format. Then, an additional MATLAB algorithm was written to extract averaged GCIPL thicknesses over displaced and nondisplaced locations, as described above, with the foveal location automatically detected from data in corresponding extensive markup language files (XML; Fig. 2).

Statistical Analysis

To compare sensitivity and specificity of displacement versus no displacement, data points were classified using the pattern deviation probability data from VFs and extracted deviation map data from OCT:

- True positive: VF location defective and OCT location defective.
- False positive: VF location not defective and OCT location defective.

- False negative: VF location defective and OCT not defective.
- True negative: VF location not defective and OCT location not defective.

Global sensitivities and specificities were computed from these classifications, and 95% confidence intervals were calculated as described by Ying et al.[21] to enable comparisons between displacement and no displacement methods. Data were also pooled as per VF clusters described by Choi et al.,[22] where VF locations falling within the same cluster demonstrate similar central tendency and distribution characteristics (see Fig. 1), to visualize potential eccentricity-dependent variations in sensitivity and specificity. By avoiding a priori assumptions regarding which locations demonstrate similar statistical characteristics, this approach provides more robust justification for pooling certain data points together, improving discriminability of trends in datasets.[23–25] An advantage of this method is that it specifically describes clusters with similar functional change characteristics across the 10-2 test grid. Unlike more widely known methods clustering locations within 24-2 test grids, such as the Garway-Heath map,[26] due to the relative sparsity of test locations there would be some ambiguity in applying the Garway-Heath map to 10-2 locations.

Further statistical analyses were performed using GraphPad Prism version 8.4.3 (GraphPad, La Jolla CA) and RStudio version 1.2.5042 (RStudio, Boston MA). As pattern deviation probability data may not entirely characterize the depth of VF loss, particularly with more severe defects, analyses using quantitative pattern deviation data were performed. Normality was assessed using D'Agostino and Pearson tests, with parametric or nonparametric tests subsequently applied as per results of these tests. Data

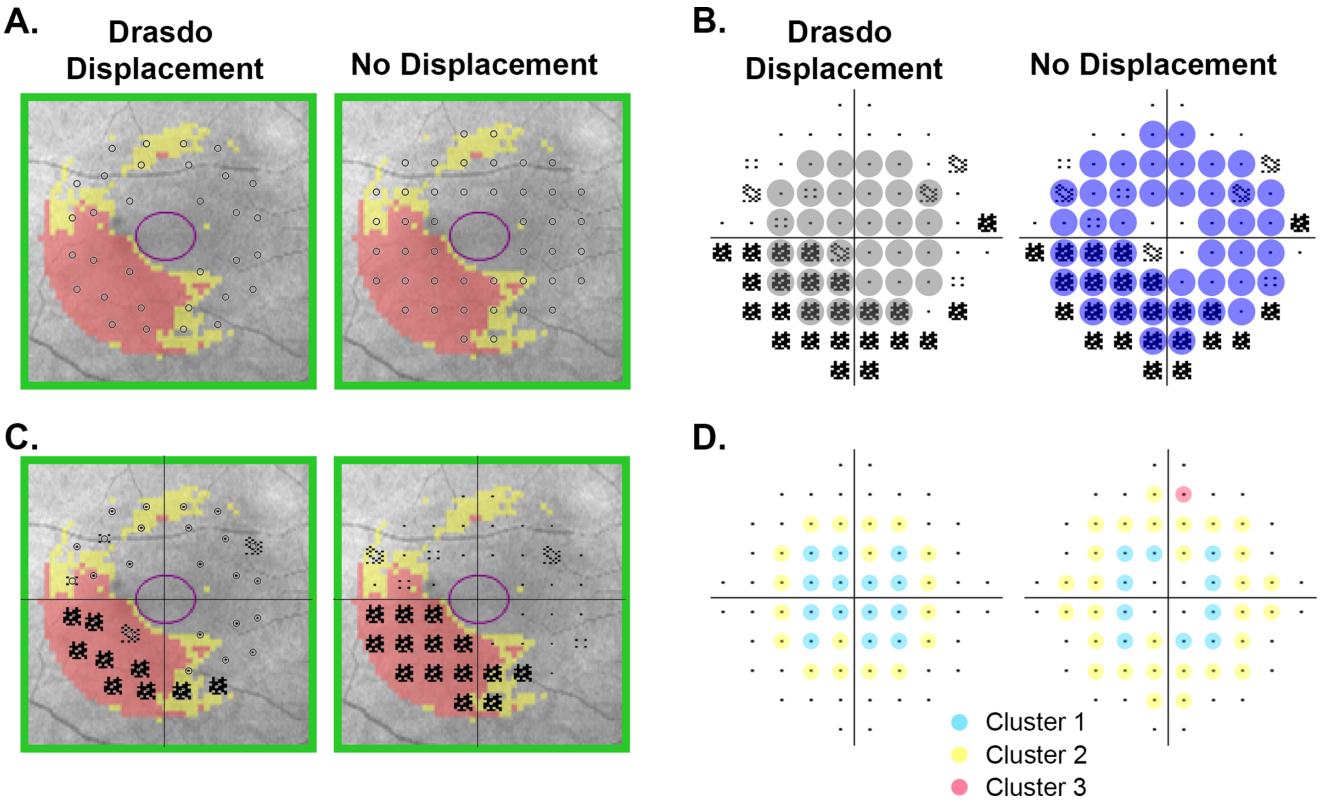

Figure 1. Extraction of OCT data from Ganglion Cell Analysis (GCA) deviation maps and 10-2 VF data with and without application of Drasdo displacement, with data from an example participant shown. All data are displayed in right eye and VF format. (**A**) Averaged color pixel values were extracted from areas enclosed by the *small circles*. (**B**) The corresponding 10-2 pattern deviation probability map. Locations were extracted from the *grey shaded areas* for Drasdo displacement and the *blue shaded areas* for no displacement. (**C**) VF data superimposed onto the deviation map, depicting the corresponding VF and OCT locations compared in later analyses. (**D**) The 10-2 VF clusters, per Choi et al.,[22] showing locations over which data were pooled for cluster-based analyses, with cluster 1 being the most central and cluster 3 being most peripheral. Note that comparisons between Drasdo and no displacement could not be performed for cluster 3 as these did not fall within the GCA measurement area with Drasdo displacement.

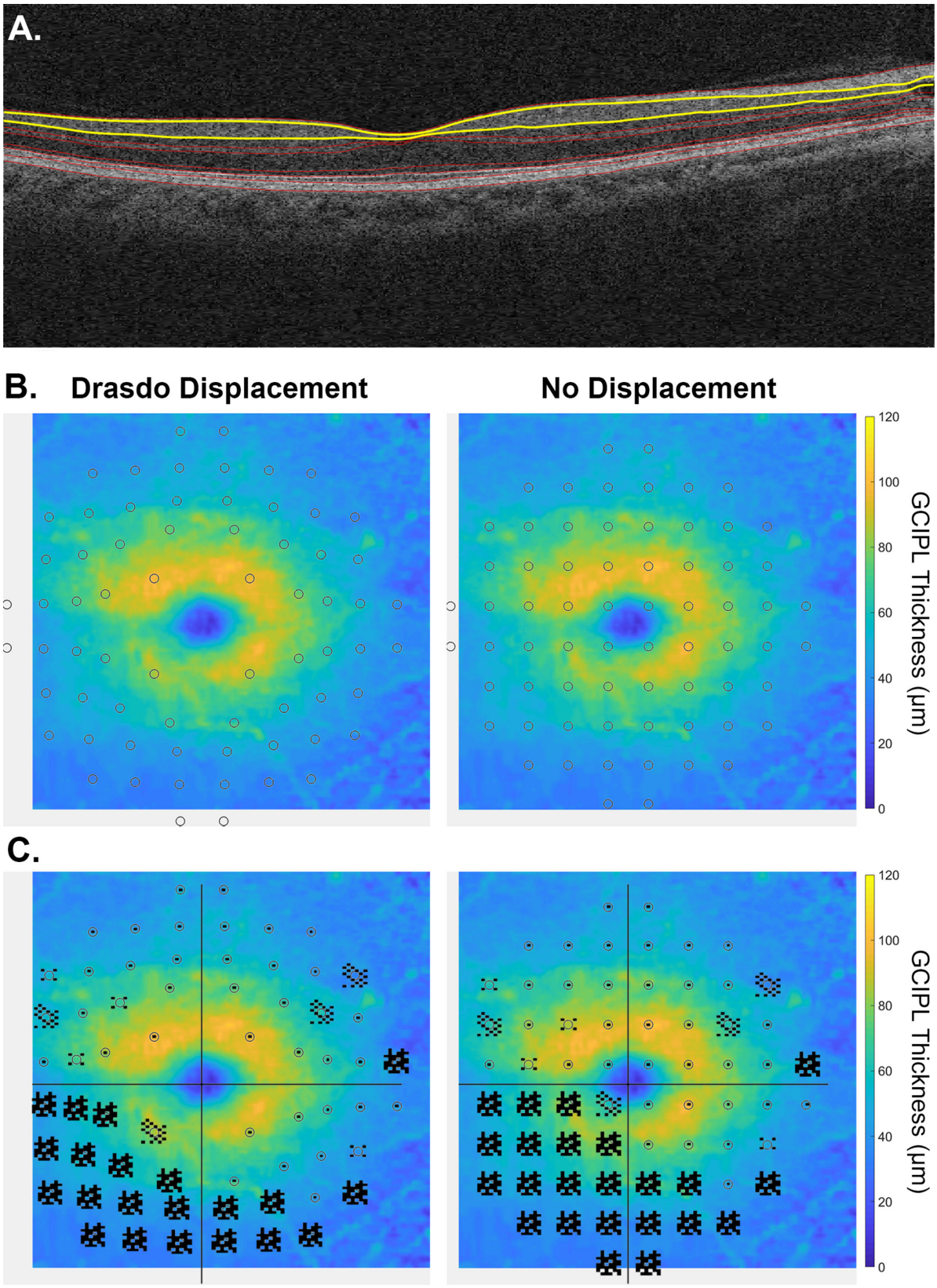

Figure 2. Extraction of raw GCIPL thickness measurements from Cirrus OCT, with data from the same participant as Figure 1 shown. (**A**) Segmentation of retinal boundaries for the foveal B-scan as performed by OCT Segmentation software, with the boundaries of the GCIPL highlighted in *yellow*. (**B**) The resultant GCIPL thickness maps, from which averaged GCIPL thicknesses were extracted in microns (μm) over areas enclosed by the *small circles*. Circles that did not fall completely on the GCIPL thickness maps were excluded from further analyses. (**C**) Pattern deviation probability data superimposed onto the GCIPL thickness maps, depicting the corresponding VF and OCT locations compared in later analyses.

across the entire cohort were categorized as VF defective or not defective, and within each category and for each pattern deviation value, the proportion of corresponding OCT locations flagged as defective versus not defective were calculated for displacement and no displacement methods. Paired *t*-tests were performed to examine OCT classifications between methods across all pattern deviation values. Differences in proportions flagged between displacement and no displacement were also plotted for each pattern deviation value, with Spearman correlations applied to investigate variations in model performance with different pattern deviation values.

Finally, for comparison of GCIPL thickness measurements and quantitative pattern deviation data, GCIPL measurements from displaced and nondisplaced locations were converted to a decibel (dB) scale to match VF data.[23,27] As linear relationships between structural and VF data have been previously reported when both are expressed in logarithmic units,[28] linear regression models between GCIPL thickness and pattern deviation values were computed. Although the OCT measurement floor may limit the ability of linear regression models to describe this relationship,[10] the tendency for pattern deviation values to underestimate severity of VF defects in advanced disease may negate the advantages of more complex regression models in accounting for the floor effect.[29] As such, segmented linear regression analyses were applied, with Davies' tests performed to determine whether significant differences in slopes on each side of the breakpoint existed, and therefore whether the structure-function relationship could be sufficiently described with a linear relationship.

For linear models, slopes were compared between displacement and no displacement using extra sums-of-squares F test, across all tested locations and separated into clusters as per Choi et al.,[22] per global sensitivity and specificity analyses. In clusters where Davies' tests were significant for both displacement and no displacement, this process was repeated for slopes and breakpoints of the segmented linear regression models. For all analyses, statistical significance was set at $P < 5\%$.

Results

Demographic Data

Data from 296 participants were included in this study (Table 1), with a mean age of 63.72 years. One hundred ninety-six participants demonstrated a VF defect on 10-2 testing as per HPA criteria. Using 24-2 mean deviation criteria,[16] 237 participants were classified as early glaucoma, with a mean deviation better than or equal to -5.00 dB, whereas 46 participants were classified as moderate glaucoma (mean deviation between -5.00 and -12.00 dB) and 13 participants were classified as having advanced glaucoma (mean deviation worse than -12.00 dB).

Of the total cohort, successful segmentation of raw data using OCT Segmentation software could be performed for 283 participants, with segmentation error by the software resulting in exclusion of 13 participants for these analyses.

Sensitivity and Specificity of Displacement and No Displacement Methods

Sensitivities and specificities derived across the macula and with varying eccentricity per the different clusters were computed, and comparisons between OCT deviation map data obtained with Drasdo displacement versus without displacement were performed (Table 2). With the inclusion of all data points falling on the GCA elliptical annulus, there were no significant differences in global sensitivity or specificity between Drasdo and no displacement, however with separation into VF clusters per Choi et al.[22] a small but significant improvement in specificity was found without displacement in cluster 2, the mid-peripheral cluster. However, this effect disappeared when including only data points that fell within the GCA annulus for both Drasdo and no displacement, but overall specificity was slightly better with no displacement when analyzing these locations only. This suggests overall better specificity with no displacement compared with Drasdo displacement, although the small magnitude of difference is unlikely to be

Table 1. Demographic Characteristics of the Study Cohort

Age, years	Sex, M:F	Eye Included, OD:OS	Spherical Equivalent D	24-2 MD dB	24-2 PSD dB	10-2 MD dB	10-2 PSD d)
63.72 ± 11.57	180:116	152:144	−1.36 ± 2.99	−3.32 ± 4.24	4.02 ± 3.12	−2.82 ± 3.78	3.15 ± 3.64

Quantitative data are displayed as mean ± standard deviation.
M, male; F, female; OD, right eye; OS, left eye; D, diopters; MD, mean deviation; dB, decibels; PSD, pattern standard deviation.

Table 2. Sensitivity and Specificity Data, With 95% Confidence Intervals Displayed in Brackets

	Overall	Cluster 1	Cluster 2	Cluster 3
All data				
Sensitivity				
Drasdo displacement	0.77 (0.75–0.80)	0.79 (0.75–0.83)	0.77 (0.74–0.79)	N/A
No displacement	0.76 (0.75–0.78)	0.79 (0.74–0.83)	0.76 (0.74–0.79)	0.67 (0.58–0.77)
Specificity				
Drasdo displacement	0.59 (0.58–0.60)	0.59 (0.58–0.61)	0.58 (0.56–0.59)*	N/A
No displacement	0.61 (0.60–0.61)	0.61 (0.59–0.63)	0.61 (0.60–0.62)*	0.39 (0.32–0.46)
Only shared locations				
Sensitivity				
Drasdo displacement	0.78 (0.75–0.80)	0.81 (0.76–0.85)	0.77 (0.74–0.79)	N/A
No displacement	0.78 (0.76–0.81)	0.79 (0.74–0.83)	0.78 (0.75–0.81)	N/A
Specificity				
Drasdo displacement	0.58 (0.57–0.59)*	0.59 (0.57–0.61)	0.58 (0.56–0.59)	N/A
No displacement	0.61 (0.59–0.62)*	0.61 (0.59–0.63)	0.60 (0.59–0.62)	N/A

*Asterisks indicated paired comparisons between Drasdo and no displacement where 95% confidence intervals do not overlap, that is a significant difference in values exist between methods. Clusters refer to VF clusters per Choi et al.,[22] with cluster 1 being the most central and cluster 3 being most peripheral. As fewer peripheral points fell within the Ganglion Cell Analysis elliptical annulus with Drasdo displacement, no locations fell within cluster 3, and therefore comparisons with no displacement could not be performed.

N/A, not applicable.

clinically meaningful. Additional analyses comparing pattern deviation values from false positive locations using Drasdo and no displacement revealed median values of -1.00 dB in both with no significant difference in distributions ($P = 0.27$, Mann-Whitney test), suggesting that a more lenient statistical criterion for identifying VF locations as defective would not notably improve specificity values.

OCT Deviation Map Data and Pattern Deviation Results

Quantitative pattern deviation data were analyzed to examine differences in concordance between Drasdo and no displacement with varying VF defect levels across the entire cohort. With data separated by VF defective and not defective classifications, with all data points considered there were no significant differences in proportions of correct classifications with Drasdo and no displacement across pattern deviation values ($P = 0.77$ and 0.33 for VF defective and not defective, respectively; Fig. 3). However, a significant correlation was observed in VF defective analyses but not for VF not defective analyses ($r = 0.40$, $P = 0.02$ and $r = 0.49$, $P = 0.08$, respectively), suggesting that performance of Drasdo and no displacement paradigms vary with worsening pattern deviation values. Similar findings were observed with data separated into central and mid-peripheral locations per clusters 1 and 2[22] (Supplementary Fig. S1).

However, upon restricting analyses to data points falling within the GCA elliptical annulus with and without Drasdo displacement, there was a significantly higher proportion of correct classifications with no displacement for VF defective locations ($P = 0.008$) and a significant correlation with worsening pattern deviation ($r = 0.50$, $P = 0.002$). For VF not defective analyses, there were no significant differences between Drasdo and no displacement, nor significant correlations with varying pattern deviation ($P = 0.09$ and $r = 0.23$, $P = 0.43$, respectively). Separation of data into VF clusters revealed locations in cluster 2 primarily drive the greater concordance between VF defective results and OCT findings (Supplementary Fig. S2). Additionally, at these mid-peripheral macular locations, a higher proportion of correct classifications was observed with VF not defective data, in contrast to the overall data ($P = 0.04$).

GCIPL Thickness and Pattern Deviation Results

Analysis of quantitative GCIPL and VF data enabled comparisons of regression models between structure and function across the entire 10-2 VF test grid. Globally, there were no significant differences

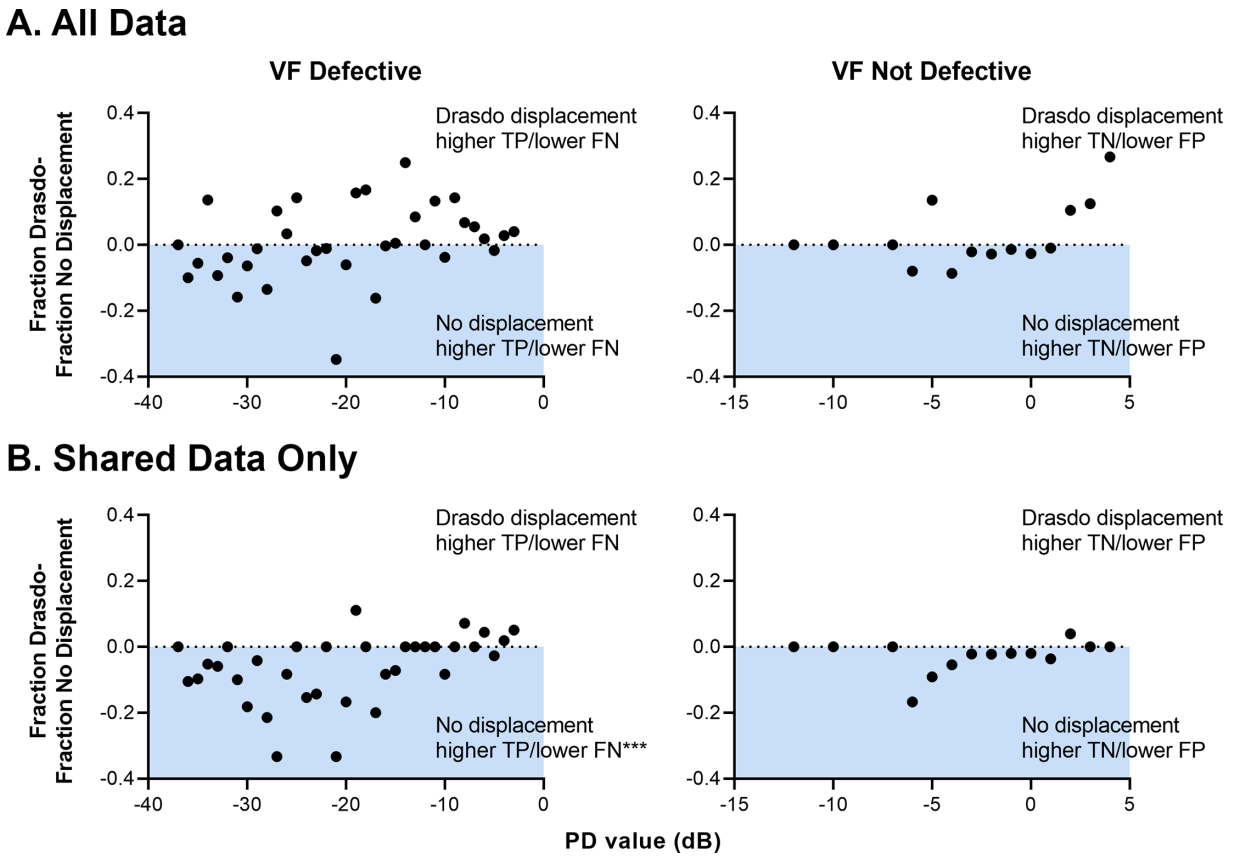

Figure 3. Performance of Drasdo displacement versus no displacement as a function of pattern deviation (PD) VF results across the entire cohort, expressed as the difference between proportions of concordant OCT and VF results (flagged as OCT defective with VF defective and as OCT not defective with VF not defective), for (**A**) all data points and (**B**) only data points included for both Drasdo and no displacement analyses. For all graphs, *unshaded areas* indicative positive differences, that is where Drasdo displacement demonstrated better concordance, whereas *blue shaded areas* indicate negative differences, that is where no displacement demonstrated better concordance. Asterisks indicate significant differences in concordance between Drasdo and no displacement ($P = 0.0008$).

in the slopes and breakpoints of both linear and segmented linear regression models with OCT data extracted over locations with and without Drasdo displacement applied (Table 3, Fig. 4). However, with data pooled per cluster 1, that is over the central macular locations, the overall slope of the linear models was significantly steeper with Drasdo displacement compared to no displacement. This indicates better concordance between GCIPL measurements and pattern deviation data with Drasdo displacement centrally. Although slope 2 of the segmented linear regression models also appeared significantly steeper with Drasdo displacement, the segmented regression model for no displacement was no better than the linear regression model ($P = 0.31$). There were no differences in slopes and breakpoints with data pooled per clusters 2 and 3, that is over mid-peripheral and peripheral macular locations, in contrast to deviation map analyses where significantly better concordance was found in cluster 2 without Drasdo displacement.

Discussion

In this study, comparing structural data from the Cirrus HD-OCT GCA and 10-2 VFs, there was slightly better macular structure-function concordance without the application of Drasdo displacement when using percentile-based OCT data in the included glaucoma cohort, as indicated by significantly higher specificities and a greater proportion of correct classifications at VF defective locations. This implies that when analyzing OCT results using normative database comparisons, as per reports readily available to clinicians, there is unlikely to be a notable clinical benefit of applying RGC displacement in interpretations of structure-function concordance. However, application of Drasdo displacement provides better concordance between GCIPL thickness and pattern deviation values at the central macula, suggesting that including RGC displacement at these locations in comparisons of

Table 3. Slope and Breakpoint Parameters for Linear and Segmented Linear Regression Models Through Pattern Deviation Data as a Function of GCIPL Thicknesses, Extracted Over Locations With Drasdo Displacement Applied and Without Displacement

	Overall	Cluster 1	Cluster 2	Cluster 3
Linear regression				
Slope				
Drasdo displacement	0.048	0.047	0.035	0.025
No displacement	0.045	0.034	0.039	0.025
P value	0.21	0.04*	0.36	0.90
R^2				
Drasdo displacement	0.051	0.051	0.047	0.065
No displacement	0.040	0.010	0.046	0.069
Segmented linear regression				
Slope 1				
Drasdo displacement	0.00007	0.012	0.0038	0.0036
No displacement	−0.00056	−0.11	−0.0020	0.0068
Breakpoint				
Drasdo displacement	−9.83	−12.00	−10.00	−11.51
P value†	<0.0001*	<0.0001*	<0.0001*	0.06
No displacement	−10.76	−29.00	−10.93	−8.00
P value†	<0.0001*	0.31	<0.0001*	<0.0001*
Slope 2				
Drasdo displacement	0.122	0.087	−0.086	0.051
No displacement	0.107	0.045	−0.096	0.067
P value	0.07	N/A	0.16	N/A
R^2				
Drasdo displacement	0.069	0.057	0.060	0.079
No displacement	0.053	0.012	0.061	0.089

R^2, coefficient of determination.

Clusters refer to VF clusters per Choi et al.,[22] with cluster 1 being the most central and cluster 3 being most peripheral. The *P* values for breakpoints of segmented linear regression models indicate results of Davies' tests, whereas all other *P* values indicate results of extra sums-of-squares F tests comparing parameters between Drasdo and no displacement regression models. Not applicable (N/A) *P* values indicate those where at least one segmented linear regression model was not significant per Davies' test results, and therefore comparison between Drasdo and no displacement segmented regression models was not performed. Across all analyses, asterisks flag significant results ($P < 0.05$).

OCT-derived GCIPL thickness data and VF data may aid clinical detection of macular structure-function concordance.

Although contrary to theoretical understandings of RGC receptive field locations relative to soma positions based on retinal anatomy, the findings of this study are largely in agreement with Hirasawa et al.,[14] who used a Nidek OCT and reported slightly higher correlation coefficients for structure-function comparisons without application of RGC displacement at the majority of locations across the macula. Considering that glaucomatous structural damage at the macula typically manifests as broad arcuate defects, even in early stages of disease,[4] if defects are wider than the magnitude of displacement then similar OCT measurements will be observed regardless of whether data are extracted with displacement applied or not. In contrast, the central 4 locations of the 10-2 VF test grid coincide with locations where RGC displacement is greatest, and without displacement GCIPL thickness is likely underestimated at these locations given encroaching upon the foveal pit. This has contributed to the larger spread in data within cluster 1 at higher pattern deviation values (see Fig. 4) as well as significantly higher correlation coefficients at these locations, as previously reported.[14] Overall, the findings of the present study and Hirasawa et al.[14] appear to consistently indicate that applying RGC displace-

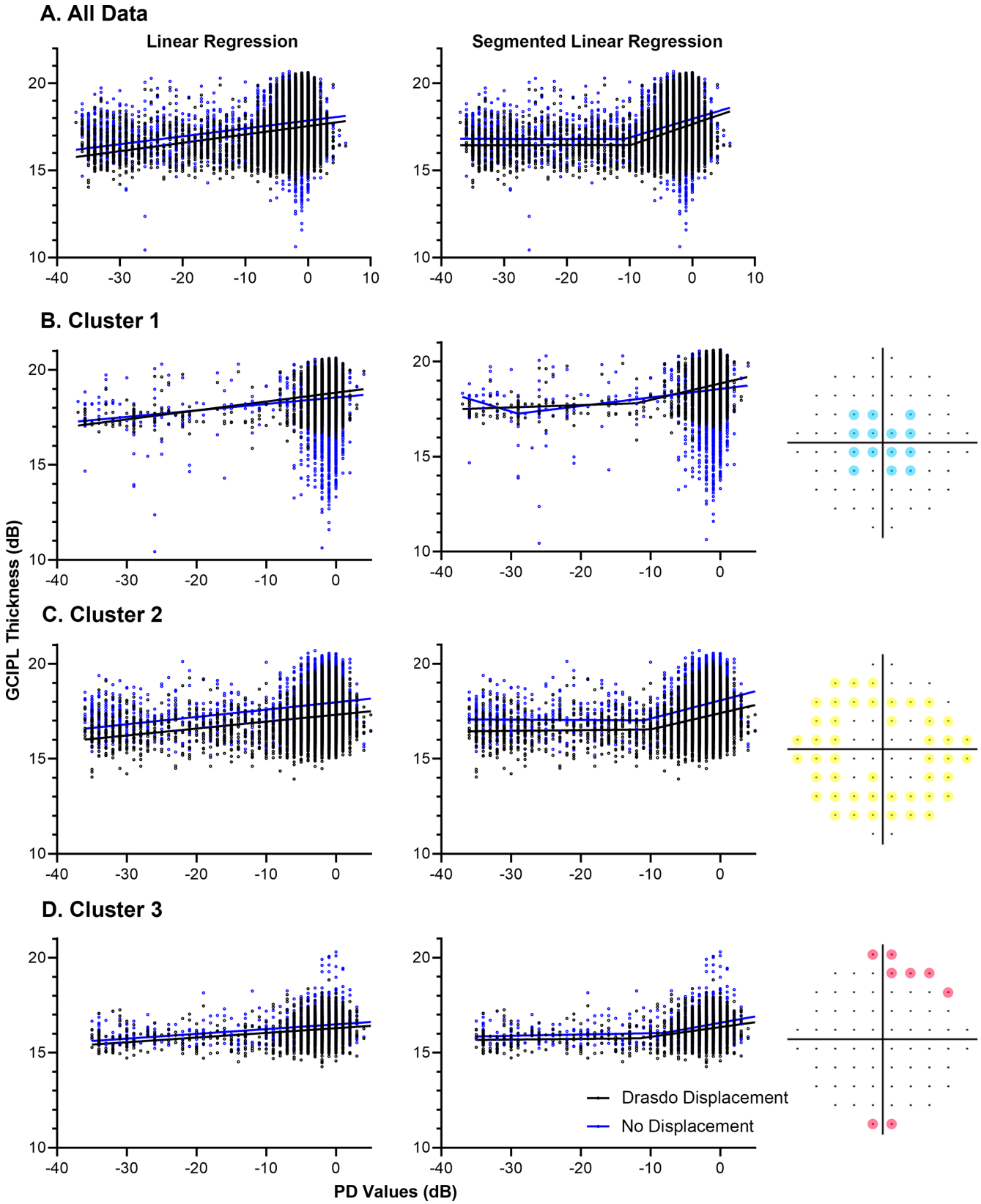

Figure 4. Linear (left column) and segmented linear (middle column) regression models through pattern deviation data as a function of GCIPL thickness, extracted over locations with Drasdo displacement applied (*black*) and without displacement (*blue*). Whereas data points are identical between the *left* and *middle* columns, regression models are shown separately for clarity. Clusters refer to VF clusters per Choi et al.,[22] with locations per cluster highlighted in the *right* column.

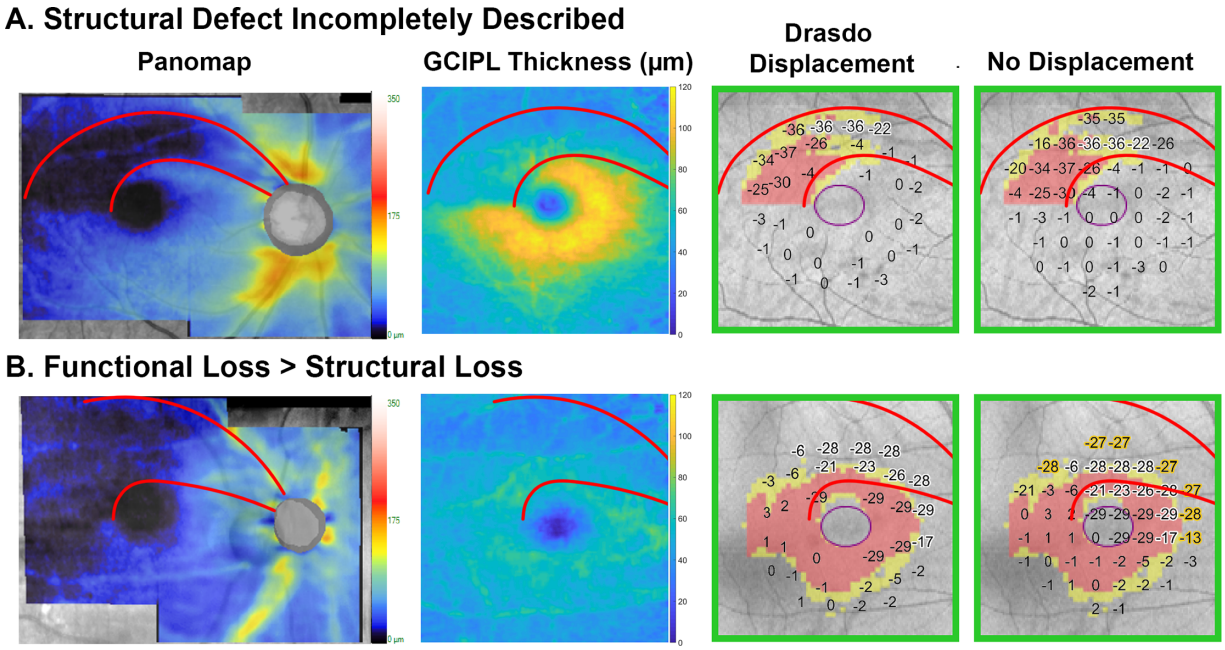

Figure 5. Data from example participants where Ganglion Cell Analysis (GCA) deviation maps did not completely describe reductions in GCIPL thickness with corresponding VF defects, resulting in apparent improved agreement with GCIPL data from non-displaced locations. Panomap data, where retinal nerve fiber layer (RNFL) and GCIPL maps are stitched together, were obtained directly from Cirrus OCT review software. Numerical data overlying the GCA deviation maps are pattern deviation data (dB). (**A**) The RNFL wedge defect (red outline) is contiguous with the optic disc from Panomap and GCIPL thickness data, but this is not reflected in the deviation map. As such, there is apparent structure-function discordance with Drasdo displacement (numbers highlighted in *white*), where the deviation map has not flagged abnormal structure within the wedge defect, although these fall within the flagged locations without displacement. (**B**) The global reduction in GCIPL thickness, more pronounced within the RNFL wedge defect (*red outline*), is not reflected by the deviation map, which has flagged more marked loss centrally. As such, there is apparent structure-function discordance with Drasdo displacement at relatively peripheral locations (numbers highlighted in *white*), although these fall within the flagged regions without displacement. However, this does not appear to be indicative of improved concordance without displacement, as more peripheral VF results also do not concord with GCIPL data at these locations (numbers highlighted in *orange*).

ment to central macular locations confers greater concordance with VF data, whereas limited differences in structure-function concordance are observed with and without displacement beyond the central macula.

An alternative reason for the lack of overall improvement in structure-function concordance with displacement is that the Drasdo model may overestimate displacement, especially outside of the central 4 locations of the 10-2 VF grid. Other histological studies have measured smaller peak displacements and magnitudes of displacement with increasing eccentricity,[30,31] with differences in studies attributed to differences in samples and shrinkage. This possibility is suggested by slightly improved correlations with VF results when using the Sjostrand RGC displacement model over the Drasdo model, although no displacement still produced better correlation coefficients overall.[14] Another possibility is that these displacement models, based on histological data obtained from a few participants only, may not account for individual differences in RGC position. Customized displacement dependent on individual data, as suggested by Turpin et al.,[32] may be required to obtain better concordance between structure and function. Further investigations regarding different RGC displacement models and the role of customizing displacement on structure-function analyses may help to elucidate the most appropriate method to apply moving forward.

Interestingly, the better agreement between OCT data from GCA deviation maps without displacement and VF data appeared to be driven by the mid-peripheral macular locations, where relatively little displacement is observed compared to the central macula. Upon further investigation, this finding appeared to be driven by participants where the GCA deviation map did not flag locations as outside of normative limits, despite visible reductions in GCIPL thickness apparent on raw data (Fig. 5). The notion that the apparently superior structure-function concordance without displacement is an artifact of errors in identifying abnormal OCT measurements is supported

by the similarities in regression models between Drasdo and no displacement at the mid-peripheral macula (see Table 3, Fig. 4). Inbuilt normative databases do not incorporate a whole host of variables affecting inter-individual variations in GCIPL thickness, including but not limited to spherical equivalent refractive error and position of the optic disc relative to the fovea related to differences in trajectory of the papillomacular fibers,[33–35] which can translate to errors as highlighted in these examples. These findings highlight the pitfalls of overreliance on comparisons to normative databases, and reinforce the importance of interpreting these in conjunction with raw OCT data to arrive at accurate clinical assessments of pathological OCT findings.

Although 10-2 VF data were used to compare structure-function concordance with and without Drasdo displacement, these findings do not necessarily indicate the ability of VF testing to accurately identify glaucomatous damage. Indeed, in cases of pre-perimetric glaucoma, discordance between structural damage consistent with glaucoma and apparently clear VFs is often observed.[3,36] The findings from this study suggest that structure-function concordance can improve when using quantitative OCT and VF data at central locations, however, it is also possible that properties of central VF test parameters are suboptimal for more precise comparisons to structural measures. Previous studies have identified that using stimulus sizes scaled to spatial summation properties can improve concordance between structure and function in normal and glaucoma participants,[11,12,37,38] which may be more pertinent in the context of the macular structure-function relationship. Further investigations on optimizing VF testing parameters could improve methods of detecting structure-function concordance in clinical settings, which would be highly valuable.

As this study used retrospective clinical data, only a single VF result per participant was used for comparison with OCT data, and there is a possibility that these results would not be repeatable. However, as only 1 VF result per eye is generally obtained in clinical settings, the judgments of the presence or absence of structure-function concordance applied in this study would more closely approximate clinical decision making. Additionally, due to the patient demographic at the Centre for Eye Health, the majority of participants included in this study have early glaucoma per mean deviation criteria, and a more even spread across different severities would be ideal to more holistically describe effects across the spectrum of glaucoma. Given the current theory that little advantage is afforded with displacement due to the width of glaucomatous defects, there may be little difference, but nonetheless confirming the effects of displacement on structure-function analyses in more cases of moderate to advanced glaucoma would be valuable.

This study has demonstrated no clinically meaningful difference between GCIPL information extracted over locations with and without Drasdo displacement applied on comparisons with 10-2 VF data in a cohort of patients with glaucoma, when using OCT data categorized according to comparisons to normative data. However, with quantitative GCIPL thicknesses, significantly better relationships between structure and function were observed at the central macula. In turn, there appears to be little clinical value in applying displacement on probability-based reports of structure and function, however, with quantitative data applying displacement may improve detection of structure-function concordance. These findings may help guide frameworks to aid appraisals of the structure-function relationship in clinical settings.

Acknowledgments

Supported by the National Health and Medical Research Council of Australia Ideas Grant (NHMRC 1186915) and an Australian Government Research Training Program Scholarship (J.T.). Additionally, Guide Dogs NSW/ACT provided a PhD scholarship (J.T.), salary support (J.P. and M.K.) and support clinical service delivery at the Centre for Eye Health. The funding bodies had no role in the conceptualization or writing of the paper.

The authors would like to thank Barbara Zangerl for involvement in discussions on project direction and Daniel Rafla for assistance in data collection.

Disclosure: **J. Tong,** None; **J. Phu,** None; **D. Alonso-Caneiro,** None; **S.K. Khuu,** None; **M. Kalloniatis,** None

References

1. Jonas JB, Aung T, Bourne RR, Bron AM, Ritch R, Panda-Jonas S. Glaucoma. *The Lancet*. 2017;390(10108):2183–2193.
2. Iyer J, Vianna JR, Chauhan BC, Quigley HA. Toward a new definition of glaucomatous optic neuropathy for clinical research. *Curr Opin Ophthalmol*. 2020;31(2):85–90.

3. Phu J, Khuu SK, Yapp M, Assaad N, Hennessy MP, Kalloniatis M. The value of visual field testing in the era of advanced imaging: Clinical and psychophysical perspectives. *Clin Exp Optom*. 2017;100(4):313–332.
4. Hood DC, Slobodnick A, Raza AS, De Moraes CG, Teng CC, Ritch R. Early glaucoma involves both deep local, and shallow widespread, retinal nerve fiber damage of the macular region. *Invest Ophthalmol Vis Sci*. 2014;55(2):632–649.
5. Phu J, Kalloniatis M. Comparison of 10-2 and 24-2C test grids for identifying central visual field defects in glaucoma and suspect patients. *Ophthalmology*. 2021;128(10):1405–1416.
6. Yamazaki Y, Sugisaki K, Araie M, et al. Relationship between vision-related quality of life and central 10 degrees of the binocular integrated visual field in advanced glaucoma. *Sci Rep*. 2019;9(1):14990.
7. Blumberg DM, De Moraes CG, Prager AJ, et al. Association between undetected 10-2 visual field damage and vision-related quality of life in patients with glaucoma. *JAMA Ophthalmol*. 2017;135(7):742–747.
8. Drasdo N, Millican CL, Katholi CR, Curcio CA. The length of Henle fibers in the human retina and a model of ganglion receptive field density in the visual field. *Vis Res*. 2007;47(22):2901–2911.
9. Hood DC, Tsamis E, Bommakanti NK, et al. Structure-function agreement is better than commonly thought in eyes with early glaucoma. *Invest Ophthalmol Vis Sci*. 2019;60(13):4241–4248.
10. Miraftabi A, Amini N, Morales E, et al. Macular SD-OCT outcome measures: Comparison of local structure-function relationships and dynamic range. *Invest Ophthalmol Vis Sci*. 2016;57(11):4815–4823.
11. Tong J, Phu J, Khuu SK, et al. Development of a spatial model of age-related change in the macular ganglion cell layer to predict function from structural changes. *Am J Ophthalmol*. 2019;208:166–177.
12. Yoshioka N, Zangerl B, Phu J, et al. Consistency of structure-function correlation between spatially scaled visual field stimuli and in vivo OCT ganglion cell counts. *Invest Ophthalmol Vis Sci*. 2018;59(5):1693–1703.
13. Raza AS, Cho J, De Moraes CG, et al. Retinal ganglion cell layer thickness and local visual field sensitivity in glaucoma. *Arch Ophthalmol*. 2011;129(12):1529–1536.
14. Hirasawa K, Matsuura M, Fujino Y, et al. Comparing structure-function relationships based on Drasdo's and Sjostrand's retinal ganglion cell displacement models. *Invest Ophthalmol Vis Sci*. 2020;61(4):10.
15. Phu J, Khuu SK, Agar A, Domadious I, Ng A, Kalloniatis M. Visualizing the consistency of clinical characteristics that distinguish healthy persons, glaucoma suspect patients, and manifest glaucoma patients. *Ophthalmol Glaucoma*. 2020;3(4):274–287.
16. Mills RP, Budenz DL, Lee PP, et al. Categorizing the stage of glaucoma from pre-diagnosis to end-stage disease. *Am J Ophthalmol*. 2006;141(1):24–30.
17. Hodapp E, Parrish RK, Anderson DR. *Clinical decisions in glaucoma*. Maryland Heights, MO: Mosby Incorporated; 1993.
18. Tong J, Alonso-Caneiro D, Kalloniatis M, Zangerl B. Custom extraction of macular ganglion cell-inner plexiform layer thickness more precisely colocalizes structural measurements with visual fields test grids. *Sci Rep*. 2020;10(1):18527.
19. Drasdo N, Fowler CW. Non-linear projection of the retinal image in a wide-angle schematic eye. *Br J Ophthalmol*. 1974;58:709–714.
20. Lang A, Carass A, Hauser M, et al. Retinal layer segmentation of macular OCT images using boundary classification. *Biomed Opt Express*. 2013;4(7):1133–1152.
21. Ying GS, Maguire MG, Glynn RJ, Rosner B. Calculating sensitivity, specificity, and predictive values for correlated eye data. *Invest Ophthalmol Vis Sci*. 2020;61(11):29.
22. Choi AYJ, Nivison-Smith L, Phu J, et al. Contrast sensitivity isocontours of the central visual field. *Sci Rep*. 2019;9(1):11603.
23. Yoshioka N, Zangerl B, Nivison-Smith L, et al. Pattern recognition analysis of age-related retinal ganglion cell signatures in the human eye. *Invest Ophthalmol Vis Sci*. 2017;58(7):3086–3099.
24. Phu J, Khuu SK, Nivison-Smith L, et al. Pattern recognition analysis reveals unique contrast sensitivity isocontours using static perimetry thresholds across the visual field. *Invest Ophthalmol Vis Sci*. 2017;58(11):4863–4876.
25. Tong J, Phu J, Kalloniatis M, Zangerl B. Modeling changes in corneal parameters with age: Implications for corneal disease detection. *Am J Ophthalmol*. 2020;209:117–131.
26. Garway-Heath DF, Poinoosawmy D, Fitzke FW, Hitchings RA. Mapping the visual field to the optic disc in normal tension glaucoma eyes. *Ophthalmology*. 2000;107(10):1809–1815.
27. Harwerth RS, Carter-Dawson L, Smith EL, 3rd, Crawford MLJ. Scaling the structure-function

relationship for clinical perimetry. *Acta Ophthalmol Scand*. 2005;83:448–455.
28. Harwerth RS, Carter-Dawson L, Smith EL, 3rd, Barnes G, Holt FH, Crawford MLJ. Neural losses correlated with visual losses in clinical perimetry. *Invest Ophthalmol Vis Sci*. 2004;45:3152–3160.
29. Asman P, Wild JM, Heijl A. Appearance of the pattern deviation map as a function of change in area of localized field loss. *Invest Ophthalmol Vis Sci*. 2004;45(9):3099–3106.
30. Sjostrand J, Popovic Z, Conradi N, Marshall J. Morphometric study of the displacement of retinal ganglion cells subserving cones within the human fovea. *Graefes Arch Clin Exp Ophthalmol*. 1999;237:1014–1023.
31. Masri RA, Grunert U, Martin PR. Analysis of parvocellular and magnocellular visual pathways in human retina. *J Neurosci*. 2020;40(42):8132–8148.
32. Turpin A, Chen S, Sepulveda JA, McKendrick AM. Customizing structure-function displacements in the macula for individual differences. *Invest Ophthalmol Vis Sci*. 2015;56(10):5984–5989.
33. Seo S, Lee CE, Jeong JH, Park KH, Kim DM, Jeoung JW. Ganglion cell-inner plexiform layer and retinal nerve fiber layer thickness according to myopia and optic disc area: a quantitative and three-dimensional analysis. *BMC Ophthalmol*. 2017;17(1):22.
34. Sezgin Akcay BI, Gunay BO, Kardes E, Unlu C, Ergin A. Evaluation of the ganglion cell complex and retinal nerve fiber layer in low, moderate, and high myopia: A study by RTVue spectral domain optical coherence tomography. *Semin Ophthalmol*. 2017;32(6):682–688.
35. Kim H, Lee JS, Park HM, et al. A wide-field optical coherence tomography normative database considering the fovea-disc relationship for glaucoma detection. *Trans Vis Sci Technol*. 2021;10(2):7.
36. Jeong JH, Park KH, Jeoung JW, Kim DM. Preperimetric normal tension glaucoma study: long-term clinical course and effect of therapeutic lowering of intraocular pressure. *Acta Ophthalmol*. 2014;92(3):e185–193.
37. Mulholland PJ, Redmond T, Garway-Heath DF, Zlatkova MB, Anderson RS. Spatiotemporal summation of perimetric stimuli in early glaucoma. *Invest Ophthalmol Vis Sci*. 2015;56(11):6473–6482.
38. Rountree L, Mulholland PJ, Anderson RS, Garway-Heath DF, Morgan JE, Redmond T. Optimising the glaucoma signal/noise ratio by mapping changes in spatial summation with area-modulated perimetric stimuli. *Sci Rep*. 2018;8(1):2172.